EBioMedicine 33 (2018) 134–143

Contents lists available at ScienceDirect

EBioMedicine

journal homepage: www.ebiomedicine.com

Research Paper

Calcium-activated Chloride Channel Regulator 1 (CLCA1) Controls Mucus Expansion in Colon by Proteolytic Activity

Elisabeth E.L. Nyström [a], George M.H. Birchenough [a], Sjoerd van der Post [a], Liisa Arike [a], Achim D. Gruber [b], Gunnar C. Hansson [a], Malin E.V. Johansson [a,*]

[a] Department of Medical Biochemistry, Institute of Biomedicine, University of Gothenburg, 40530 Gothenburg, Sweden
[b] Department of Veterinary Pathology, Freie Universität Berlin, Germany

ARTICLE INFO

Article history:
Received 23 January 2018
Received in revised form 23 May 2018
Accepted 24 May 2018
Available online 7 June 2018

Keywords:
mClca3
Gob-5
Asthma
COPD
Colon
MUC2

ABSTRACT

Many epithelial surfaces of the body are covered with protective mucus, and disrupted mucus homeostasis is coupled to diseases such as ulcerative colitis, helminth infection, cystic fibrosis, and chronic obstructive lung disease. However, little is known how a balanced mucus system is maintained. By investigating the involvement of proteases in colonic mucus dynamics we identified metalloprotease activity to be a key contributor to mucus expansion. The effect was mediated by calcium-activated chloride channel regulator 1 (CLCA1) as application of recombinant CLCA1 on intestinal mucus in freshly dissected tissue resulted in increased mucus thickness independently of ion and mucus secretion, but dependent on its metallohydrolase activity. Further, CLCA1 modulated mucus dynamics in both human and mouse, and knock-out of CLCA1 in mice was compensated for by cysteine proteases. Our results suggest that CLCA1 is involved in intestinal mucus homeostasis by facilitating processing and removal of mucus to prevent stagnation. In light of our findings, we suggest future studies to investigate if upregulation of CLCA1 in diseases associated with mucus accumulation could facilitate removal of mucus in an attempt to maintain homeostasis.

1. Introduction

The nonkeratinized epithelial surfaces in the body are covered with protective mucus with different composition and properties depending on location. Changes in mucus properties are associated with diseases such as ulcerative colitis (UC), helminth infections, cystic fibrosis (CF), asthma, and chronic obstructive lung disorder (COPD), (reviewed in [1–4]). For example, thick and stagnant mucus is a major pathology in asthma, COPD and CF, whereas UC is associated with decreased barrier function of colonic mucus [1]. Thus, knowledge of factors regulating mucus properties is important for understanding of the aforementioned diseases.

The colonic mucus is a crucial first line of defense against bacteria in addition to serving as lubricative gel [5]. The main structural component of the intestinal mucus is mucin 2 (MUC2) which, after polymerization and secretion, forms a dense network on the epithelial surface in the colon [6]. This inner mucus layer is impenetrable to most bacteria that reside in the gut and thus creates a protective barrier against infection [5]. The epithelium responds to disruption of the inner mucus layer with increased mucus secretion to restore its barrier function [7] but prolonged disturbances in the inner mucus layer are linked to colitis [8, 9].

Newly secreted mucus pushes the preformed inner layer towards the lumen, and the inner mucus layer is converted into a looser outer mucus layer by expansion of the structure. This renders the outer mucus more accessible to the intestinal microbiota [5]. The expansion is suggested to be 3–4 fold and mediated by proteolysis, but the enzymes involved are not known. In germ free (GF) animals mucus layer formation is divergent from conventionally raised mice, but the presence of a loose mucus layer in the GF colon implies endogenous enzymes to be involved in mucus processing [5, 10]. In the small intestine the importance of mucus proteolysis has been shown by the involvement of the protease meprin β, which is responsible for mucus release from the epithelium [11]. Mucus homeostasis is however not only dependent on proteolysis, but maintained by balanced production, secretion and proteolysis of mucus components. Further, mucus homeostasis is also dependent on the ionic milieu it is secreted into, as seen in the small intestine of mice that lack a functional CFTR ion channel where mucus remains attached due to lack of bicarbonate secretion [5, 6, 11, 12]. Problems with stagnant mucus in the intestine are also relevant for CF patients with meconium ileus [3]. However, the mechanisms for maintenance of colonic mucus dynamics and their importance for a functional mucus layer remain poorly understood.

* Corresponding author at: Department of Medical Biochemistry, Institute of Biomedicine, University of Gothenburg, Box 440, SE-405 30 Gothenburg, Sweden.
E-mail address: malin.johansson@medkem.gu.se (M.E.V. Johansson).

https://doi.org/10.1016/j.ebiom.2018.05.031

Calcium-activated chloride channel regulator 1 (CLCA1, previously mClca3 or Gob-5 in mouse) is primarily expressed in the intestines (Human protein atlas 180306) and is highly abundant in intestinal mucus [5, 13, 14], it has however also been detected at low levels in other mucosal tissues such as uterus, testis and kidney [15]. High degree of conservation between human and murine CLCA1 (75% identity, 93% similarity by UNIPROT alignment) suggest functional conservation. CLCA1 was initially observed to alter calcium-activated chloride currents (I_{CaCC}) over cell membranes when expressed *in vitro*. Since the observation that CLCA1 is a secreted protein, it has been believed that CLCA1 exerts this effect by regulating calcium activated chloride channels (CaCCs) [16–20]. Additionally, CLCA1 has an N-terminal zinc-dependent metallohydrolase domain with a conserved HExxE catalytic motif similar to that found in matrix metalloproteases (MMPs), and "a Disintegrin and metalloproteases" (ADAMs) [18, 21, 22]. The only known substrate for CLCA1 is CLCA1 itself as it undergoes intracellular autocatalytic cleavage resulting in two cleavage products which are both secreted [20]. The proteolytic and ion current related activities of CLCA1 make it an interesting candidate for regulation of mucus dynamics and homeostasis. In addition CLCA1 is upregulated in the lungs (where it is not normally expressed) during asthma, COPD and CF with a suggested role in T_H2 driven mucus production with implications for severity of these diseases [23].

Previous studies of Clca1-deficient mice did not show any intestinal specific phenotypes in terms of mucus barrier function under naïve or dextran sodium sulfate (DSS) treatment conditions [13, 24, 25]. Further, alterations in mucin expression, compensatory expression of CLCA1 paralogs or alterations in microbiota composition were not found which could otherwise have partly explained the lack of phenotype. Nonetheless, the high abundance of CLCA1 in intestinal mucus still indicates a functional role in this context that was not detected with the methods previously used.

Here we have employed an approach that allows studies of the intestinal mucus layer *ex vivo* in combination with pharmacological interventions to investigate the involvement of endogenous proteases in colonic mucus dynamics [7, 11, 26, 27]. As we identified a role for metalloprotease activity, we further investigated the function of CLCA1 in mucus. This was achieved by measuring alterations in colonic mucus dynamics after treatment with recombinantly expressed and purified CLCA1 (rCLCA1), alone or in combination with inhibitors. We found that the proteolytic activity of CLCA modulates baseline mucus dynamics, independently of ion or mucus secretion. These results suggest that CLCA1 is able to process and expand the mucus structure and could by this be important both for mucus homeostasis and to facilitate clearance of mucus in disease.

2. Materials and Methods

2.1. Animals

Swiss Webster germ-free mice kindly provided from F. Bäckhed (Gothenburg University, Sweden), and *Clca1*$^{-/-}$ (Clca1^{tm1Htzm}, RRID: MGI:3802573) [24] and WT mice on C57Bl/6 N background from homozygote breedings were used in full compliance according to Swedish animal welfare legislation and approved by the Swedish Laboratory Animal Ethical Committee in Gothenburg, Sweden (number: 280–2012 and 73–15). *Clca1*$^{-/-}$ and Conv-R WT mice were kept in a SPF facility in single ventilated cages, and germ-free animals were kept in flexible film incubators, with food and water *ad libitum* and 12 h light/dark cycles. Isoflurane was used for anesthesia followed by cervical dislocation for sacrificing of the mice. Animals of both genders were used at an age of 8–16 weeks.

2.2. Human Samples

Sigmoid colon biopsies for mucus measurements and proteomics were obtained from patients referred for colonoscopy at Sahlgrenska University Hospital, Gothenburg, Sweden, in compliance with the human research ethical committee in Gothenburg, Sweden (040–08), and the Declaration of Helsinki. Patients with normal intestinal mucosa by macroscopic evaluation were included in the study after informed consent. Biopsies were obtained as described previously [26]. Mucus measurements were performed on biopsies from 7 patients (5 males, 2 females, age range: 33–71 years, median age: 61 years) and proteomic analysis was performed on mucus from 47 subjects (25 males, 22 females, age range: 23–87 years, median age: 59 years).

2.3. Proteomics

Mouse mucus proteome data was taken from WT intensities from a previously published data set (PRIDE partner repository [28], dataset identifier PXD001804) [13].

Human mucus proteome samples were collected from biopsies after one hour in a horizontal perfusion chamber [26] and were reduced, alkylated and digested with trypsin using a modified filter-aided sample preparation [29] as described before [13] with the exception of the use of a 10 kDa cut-off filter and overnight tryptic digest only. Liquid chromatography and mass spectrometry were performed as described in detail earlier [30]. MaxQuant version 1.3.0.5 [31] was used for data processing and peptide quantification, and proteins were identified by Andromeda [32]. Database searches were performed against the human SwissProt protein database (v2014_120 181 entries) with the following settings: (i) trypsin allowing one miss cleavage; (ii) precursor tolerance 7 ppm and 0.5 Da for fragment ions; (iii) fixed modifications carbamidomethyl cysteine and variable oxidized methionine and acetylated protein N-terminal. The false discovery rate for both peptide and protein identifications was set to 1% based on a minimum of one unique peptide per protein and were grouped when based on the same set of peptides. The peptide match between runs option was limited to a retention time window of 2 min.

2.4. Histology and Immunohistochemistry

Mouse and human colonic biopsies were directly fixed in methanol-Carnoy fixative, paraffin embedded and cut in 4 μm sections [5, 13]. Mouse colonic tissues that had been mounted for mucus measurement were fixed in methanol-Carnoy fixative, paraffin embedded and cut in 4 μm sections. Dewaxed and rehydrated sections were stained with Alcian blue/Periodic acid Schiff (Ab/PAS). Immunohistochemistry was performed on dewaxed, rehydrated and antigen retrieved sections using mouse monoclonal anti-CLCA1 (ab129283, Abcam, RRID:AB_11155317) and rabbit polyclonal anti-MUC2 C3 primary antibodies [5]. Alexa 546 conjugated goat anti-mouse (RRID:AB_144695) and Alexa 488-conjugated goat anti-rabbit (RRID:AB_2534069) secondary antibodies were used and Hoechst 34580 for DNA counter-stain. Images were acquired using a Nikon eclipse E1000 fluorescence microscope (Nikon) with the NIS elements software (Nikon).

2.5. Ex vivo Mucus Analysis

Tissues for *ex vivo* mucus analysis was prepared as described by Gustafsson et al. [13, 26] In brief, distal colon tissue was dissected and flushed with ice-cold Krebs' transport solution unless otherwise stated. The tissues were opened longitudinally, the longitudinal muscle layer was removed and the epithelial tissue was subsequently mounted in a horizontal Ussing chamber with basolateral Kreb's glucose solution and apical Kreb's mannitol solution. Carboxylated polystyrene beads were added to the apical buffer to visualize the mucus.

2.6. Mucus Measurement

The mucus thickness was measured at $t = 0$, 30 and 60 min after mounting, and the growth rate of the mucus was calculated from

these measurements as previously described [13, 26]. Treatment of mucus and tissue was performed just after the $t = 30$ min measurement. All treatments, except Carbachol (CCh, Sigma) and Batimastat, were applied in 50 μl Kreb's mannitol solution replacing the corresponding volume of the apical buffer. CCh was added to basolateral buffer just after t = 30 min. Due to the poor solubility of Batimastat in Kreb's mannitol buffer, it was instead dissolved in 150 μl PBS containing 0.02% Tween-20, and the entire volume of the apical buffer was replaced upon Batimastat treatment. Control measurements with mucus treated only with the dissolvent showed no difference to mucus kept in Kreb's mannitol. Human sigmoid colon biopsy samples were mounted and treated in a similar fashion as mouse tissue [26]. In general, 2–4 specimens from the same animal/patient were mounted, and each specimen used for different treatment.

Inhibitor concentrations were: Batimastat (200 μM), Bestatin (130 μM), Disodium 4,4′-diisothiocyanatostilbene-2,2′-disulfonate (DIDS, 200 μM), (2*S*,3*S*)-trans-Epoxysuccinyl-L-leucylamido-3-methylbutane (E64-c, 20 μM), ethylenediaminetetraacetic acid (EDTA, 10 mM), ethylene glycol-bis(β-aminoethyl ether)-N,N,N′,N′-tetraacetic acid (EGTA, 10 mM), Niflumic acid (NFA, 300 μM), and N,N,N′,N′-Tetrakis(2-pyridylmethyl)ethylenediamine (TPEN, 1 mM) (all from Sigma), Calcium activated chloride channel inhibitor A01 (CaCCinh A01, 100 μM) (Millipore) and cOmplete EDTA-free protease inhibitor (cOmpl, 1×) (Roche). The chosen concentrations were based on concentrations used in published studies (*in vitro* or *in vivo*), by testing the highest concentration tolerated by the tissue, and/or solubility of the drug.

2.7. Penetrability and Bead Tracking

Penetrability assay was performed as described before [13] with tissue mounted in a chamber with an oval opening (2.5*5 mm) with CellTrace Calcein Violet AM stain (1 μg/ml, Thermo Fisher) in the basolateral Kreb's glucose solution. Crimson fluorescent carboxylate-modified microspheres (1 μm, Thermo Fisher) were used for visualization of the distribution of 1 μm particles on and in the mucus. The tissue was kept at 37 °C and *Z*-stacks were recorded at 3–4 positions in each tissue at time point $t = 0$, 30 and 60 min after mounting using a LSM700 Examiner Z.1 upright confocal microscope with Plan-Apochromat ×20/1.0DIC water objective and Zen imaging software (Zeiss). Treatment with rCLCA1 was performed by removing the apical buffer after the t 30 min recordings and applying rCLCA1 diluted in Kreb's mannitol buffer to the apical surface.

Data for bead tracking analysis was recorded during penetrability assays by recording time-series (2 frames/s) in the crimson fluorescence microsphere channel at different focus planes. The mucus surface was set as position 0 and the z-plane focus was moved up in 30 μm intervals. The bead movements were recorded at 3 x/y-positions in each tissue at $t = 20$ min and at $t = 60$ min. Imaris image analysis software (version 7.6.3, Bitplane AG) was used for tracking the average bead speed in each focus plane.

2.8. Ex vivo Mucus Lectin Staining

Explants were prepared from flushed (removes loose mucus) or unflushed colonic tissue and mounted in perfusion chambers and stained with 50 μg/ml rhodamine labeled *Ulex europaeus* Agglutinin I (UEA1; Vector Laboratories, RRID:AB_2336769) diluted in Kreb's mannitol buffer which was applied to the apical tissue surface. Tissue was incubated for 15 min at room temperature and then washed twice in fresh Kreb's mannitol and imaged by confocal microscopy. The inner and outer mucus layers were stained by UEA1 and mucosal bacteria with Syto9 (Thermo Fisher) in unflushed explants from colonic tissue as previously described [33]. Quantification of mucus aggregation was performed by imaging UEA1 fluorescence over a 0.5–0.6 mm^2 area of tissue. Confocal image files were exported to Imaris image analysis software (version 7.6.3, Bitplane AG) and isosurfaces were mapped to a threshold level of UEA1 fluorescence. Total isosurface volume was quantified and normalized to tissue area. All images for quantitative comparison were taken using the same confocal image acquisition settings.

2.9. Expression and Purification of Recombinant

CLCA1 pcDNA3.1 vectors containing the human CLCA1 sequence [22] with a C-terminal His-tag with or without alterations (see below) were used for mammalian expression of recombinant CLCA1 (rCLCA1). Vectors were transiently transfected into FreeStyle CHO-S cells (RRID:CVCL_D604) and spent medium were collected at 72 h post transfection. Cells and debris was removed by centrifugation and the remaining supernatant was dialyzed against PBS. Nickel or cobalt Hi-trap columns were used for His-tag aided purification. Eluates were dialyzed to PBS and concentrated using Vivaspin 10,000 MW (Sartorius). Protein concentrations were determined with a BCA Protein Assay Kit (Pierce).

2.10. p.E157Q and p.GALY694-697DFRE Mutagenesis

A CLCA1 protease null mutant p.E157Q, and a modified cleavage site mutant p.GALY694-697DFRE [18] were generated using QuikChange Site-directed mutagenesis kit (Aglient Technologies) according to the manufacturer's instruction with 50 ng pcDNA3.1-hCLCA1-His as parental vector. p.E157Q was introduced using forward primer 5′-GGG CAT TTG TCC ATC AGT GGG CCC ATC TAC GAT GGG G -3′. The p.GALY694-697DFRE mutation was achieved in a two-step mutagenesis by first producing a p.GA695-696FR mutant using forward primer 5′- GTG ATA CCC CAG CAG AGT GGA TTC CGG TAC ATA CCT GGC TGG ATT GA -3′ followed by a mutagenesis using forward primer 5′- TGA TAC CCC AGC AGA GTG ATT TCC GGG AGA TAC CTG GCT GGA TTG AG-3′. The reverse complementary sequences to the forward primers were used as reverse primer in all cases. Purified plasmids were sequenced to confirm the mutations.

2.11. Western Blot Analysis

Mucus was collected from mouse or human colonic biopsies after removal of luminal content, by gentle scraping and was collected in Kreb's buffer containing 2× cOmpl and 250 μM N-Ethylmaleimide. Samples for gel electrophoresis and western blot analysis were reduced in DTT and run in Mini-PROTEAN TGX 4–20% gels (Bio-Rad) with SDS-containing running buffer. The proteins were blotted to PVDF membranes using a semi-dry trans-blot turbo system (Bio-Rad) with the appropriate buffers. The membrane was probed with a rabbit monoclonal anti-CLCA1 primary antibody (ab180851, Abcam, RRID:AB_2722611) at 1:10000, and a goat anti-rabbit alkaline phosphatase conjugated secondary antibody (Southern Biotech, RRID:AB_2722612) at 1:1000. Nitro-blue tetrazolium and 5-bromo-4-chloro-3′-indolyphosphate (NBT/BCIP) was used for development. Precision Plus Protein™ Dual Colour Standard (Bio-Rad) was used as molecular weight standard.

2.12. Statistical Analysis

Sample size estimation was performed using GraphPad StatMate version 2.00 for Windows (GraphPad Software), with “Compare two means” and standard deviations from previous experiments as input parameters. Statistical analysis and graphical illustrations were performed using GraphPad PRISM 7.03 (GraphPad Software). Data are presented as mean ± SEM, unless otherwise indicated. Statistical analysis of mucus growth rates was performed with *t*-test, one or two-way ANOVA with multiple comparison tests as indicated. For penetrability analysis area under curve (AUC) for each individual samples were calculated with baseline set to $Y = 0$. $P \leq 0.05$ was considered as significant.

3. Results

3.1. Endogenous Metalloproteases are Involved in Colonic Mucus Dynamics

Previous studies have suggested that endogenous proteases are involved in forming a detached outer mucus layer as a mixture of cysteine and serine protease inhibitors partly blocked mucus growth *in vivo* in rat and GF mouse, colon [5]. To further investigate the involvement of endogenous proteases in mucus growth conventionally raised (Conv-R) and GF mouse colon mucus was treated with the metalloprotease inhibitor EDTA in an *ex vivo* horizontal Ussing chamber-like system which can be used to study intestinal mucus properties and dynamics (Fig. 1a) [26]. Mucus growth was significantly inhibited in both Conv-R and GF mice, indicating the involvement of endogenous metalloproteases in controlling mucus expansion.

Analysis of the mucus proteome in both mouse and human colon identified calcium-activated chloride channel 1 (CLCA1) to be one of the most abundant proteins in mucus from both species together with albumin, actin, FCGBP and MUC2 (Fig. 1b). CLCA1 contains a metallohydrolase domain in its N-terminal part and thus is a strong potential candidate for involvement in metalloprotease-dependent mucus dynamics (Fig. 1c) [18].

Methanol-Carnoy fixed colon sections were stained for CLCA1 and MUC2 to compare Conv-R and GF mice (Fig. 1d). CLCA1 and MUC2 showed comparable staining patterns and intensities in both groups.

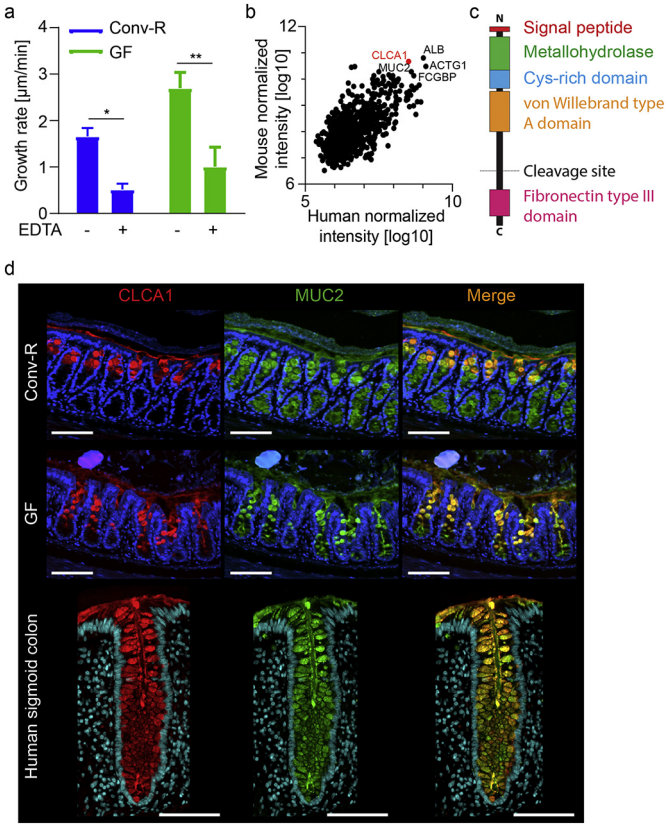

Fig. 1. CLCA1 is a candidate to be the metalloprotease involved in mucus growth in WT and GF colon. (a) Distal colon mucus growth rate measured in Conv-R and GF mice without (−) and with (+) 10 mM EDTA applied apically ($n = 4$–6). (b) Proteome analysis of mouse and human colonic mucus. The five shared most abundant proteins are labeled with their gene names. CLCA1 is marked in red (mouse $n = 7$, human $n = 47$). (c) Schematic representation of CLCA1 with marked domains. (d) Immunostainings of CLCA1 (red) and MUC2 (green) in Conv-R and GF mice, and in human sigmoid colon sections. DNA was stained with Hoechst (blue) (representative of 9–15). Scale bar is 100 µm. Data is presented as mean ± SEM; * $p \leq .05$, ** $p \leq .01$, with two-way ANOVA with Sidak's multiple comparisons test (MCT).

Human sigmoid colon sections were stained in a similar fashion, and showed a strong staining of CLCA1 in MUC2 containing goblet cells throughout the colonic crypt and could also be observed in the secreted mucus (Fig. 1d), as previously shown in mice [13].

3.2. CLCA1 Causes Increased Mucus Thickness and Penetrability in Live Tissue

To investigate if CLCA1 is involved in mucus growth, rCLCA1 was applied to mucus from WT and *Clca1*$^{-/-}$ mice *ex vivo*. rCLCA1 caused a significant increase in mucus growth rate in both genotypes (Fig. 2a). The responses were quantitatively similar, suggesting that the normal effect of CLCA1 in WT mucus is restricted and can be enhanced by exogenous application of rCLCA1.

Furthermore, mucus treated with rCLCA1 was significantly more penetrable to 1 µm beads compared to untreated controls. This was true for both *Clca1*$^{-/-}$ (Fig. 2b–d) and WT (Fig. S1a–b) mucus and indicated that the enhanced mucus growth was due to expansion of the mucus making in more penetrable. Tracking the movement of beads above the mucus surface in *Clca1*$^{-/-}$ colon revealed that rCLCA1 treatment decelerated bead movement, which remained unchanged in untreated controls (Fig. 2e and Videos S1 & S2). This effect was also observed in WT mice (Fig. S1c). Reduced bead mobility indicated increased mucus density at the mucus/liquid interface after rCLCA1 treatment. Enhanced transformation of the mucus to a more penetrable structure would indeed make the mucus density higher at the site where this process occurs, at the outer surface of the inner mucus layer.

3.3. The Effect of CLCA1 can be Inhibited by Protease Inhibitors

To investigate if the observed effect of rCLCA1 was mediated by proteolysis, rCLCA1 was applied first together with a combination of the metalloprotease inhibitor EDTA and cOmplete EDTA-free serine and cysteine protease inhibitor cocktail (cOmpl) (Fig. 3a). The combined inhibitors abolished the effect on mucus growth of rCLCA1. The contribution of each inhibitor was addressed by adding them separately. Most of the effect of rCLCA1 was blocked by EDTA, while the cOmplete EDTA-free inhibitor cocktail had no significant inhibitory effect on the induced mucus growth. Both EGTA and TPEN, which preferentially chelate Ca^{2+} and Zn^{2+} ions respectively, efficiently inhibited the effect of rCLCA1 indicating that CLCA1 is dependent on both Ca^{2+} and Zn^{2+} as has been described [18, 21]. However, neither the matrix metalloprotease inhibitor batimastat nor the exopeptidase inhibitor bestatin had any effect on the rCLCA1 treatment, suggesting that CLCA1 is an *endo*-, rather than exopeptidase.

To analyze if our results with rCLCA1 were possible to translate to the human colon, we repeated the application of rCLCA1 on *ex vivo* mountings using human colon biopsies (Fig. 3b). Application of rCLCA1 significantly increased the mucus growth indicating similar effects of rCLCA1 in human and mouse. Furthermore, EDTA treatment inhibited the endogenous mucus growth in human colon mucus. It thus appears that metalloprotease activity, likely derived from CLCA1, is important for baseline mucus growth in humans, as well as in mice.

3.4. Metallohydrolase Activity but Not Autocatalytic Cleavage of CLCA1 is Required for Activity

For further confirmation that CLCA1 was indeed acting as a metalloprotease we generated a protease null mutant of CLCA1 (CLCA1 p.E157Q) (Fig. 3c) [18, 21, 22]. Western blot (WB) analysis of purified rCLCA1 p.E157Q indicated almost complete inhibition of the autocatalytic cleavage (Fig. 3d, E157Q) (the detected product at 75 kDa is due to unspecific degradation in the sample). No increase in mucus growth rate was measured upon application of rCLCA1 p.E157Q, adding to the evidence that rCLCA1 acts as a metalloprotease in the mucus (Fig. 3e, E157Q). To exclude that the autocatalytic cleavage

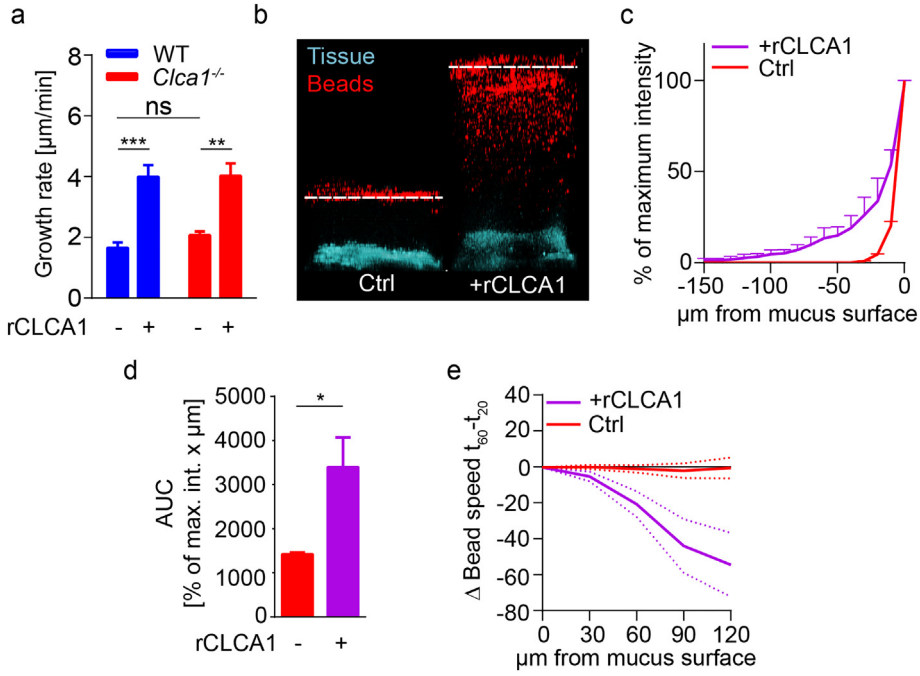

Fig. 2. CLCA1 causes increased mucus growth and penetrability in WT and *Clca1*$^{-/-}$ mice. (a) Distal colon mucus growth rate measured in WT and *Clca1*$^{-/-}$ mice without (−) and with (+) 5 μg rCLCA1 applied apically (n = 4–7). (b) Representative z-stack projections of bacteria sized bead (1 μm, red) distribution in distal colon mucus of WT and *Clca1*$^{-/-}$ at 30 min after control (PBS) treatment (left panel), or after rCLCA1 (10 μg) treatment (right panel) ($n = 8$). Dashed line indicates mucus surface. (c) Distribution of beads in control or rCLCA1 (10 μg) treated *Clca1*$^{-/-}$ mucus. The z-position with highest bead intensity was defined as the mucus surface, and the bead penetrance in the mucus was plotted as % of maximum intensity at each z-position below the mucus surface ($n = 4$). (d) Area under curve (AUC) analysis of bead penetrability data (c) comparing rCLCA1 treated with control mucus (n = 4). (e) Change in average bead speed in different z-planes above the mucus surface between $t = 20$ min and $t = 60$ min in control or rCLCA1 (10 μg) treated *Clca1*$^{-/-}$ mucus, where the treatments were applied at $t = 30$ min. Bead mobility data is shown in Videos S1 and S2 ($n = 3$–5). Data is presented as mean ± SEM; * $p \le .05$, ** $p \le .01$, *** $p \le .001$ with either two-way ANOVA with Tukey's MCT (a) or unpaired 2-tailed *t*-test (d).

of rCLCA1 was required to induce mucus growth we also generated an rCLCA1 mutant, p.GALY694-697DFRE, with a non-functional cleavage site but an intact catalytic site. The WB analysis indicated loss of cleavage of the CLCA1 mutant (Fig. 3d, DFRE). However, no difference in the delta mucus growth rate compared to the unmodified (WT) rCLCA1 was observed (Fig. 3e, DFRE).

Since a previous study suggested that the autocatalytic cleavage of CLCA1 regulates its activity [18], processing of CLCA1 *in vivo* was investigated. Mucus from human colonic biopsies as well as WT and *Clca1*$^{-/-}$ mouse colon were separated by SDS-PAGE and probed with an antibody recognizing the N-terminal cleavage product of CLCA1 (Fig. 3F). A band around 75 kDa, corresponding to the N-terminal autocatalytic cleavage product, was observed in mucus from both human and WT mouse, but not in *Clca1*$^{-/-}$ mucus. In addition, an additional band at 50 kDa was identified in human and WT mouse mucus, but not in *Clca1*$^{-/-}$ mucus, suggesting that CLCA1 can be further processed. However, no band corresponding to the full-length un-cleaved CLCA1 could be detected in the human samples, and only a very faint band was observed in WT mouse mucus, indicating that most of the CLCA1 that is secreted into the mucus is fully cleaved *in vivo*.

3.5. The Mucus Growth Stimulated by CLCA1 is Not Mediated by Secretion

Increased mucus thickness can be caused either by proteolytically mediated mucus expansion, increased mucus secretion, by alterations in the ionic milieu, or a combination thereof [5, 7, 27]. To exclude that the observed effect of rCLCA1 was due to increased mucus or ion secretion the transepithelial potential difference (PD) was recorded during rCLCA1 or control (PBS) treatment of *Clca1*$^{-/-}$ tissue. As positive control, tissues were treated with carbachol (CCh), a cholinergic agonist known to induce mucus and ion secretion. The effect on mucus growth of CCh treatment was in a similar range to that of rCLCA1 (Fig. 4a). However, in contrast to the rapid and robust PD decrease in response to CCh treatment, no PD response was evoked by rCLCA1 treatment in mouse (Fig. 4b) or human tissue (Fig. S2). These results do not support ion–transport to be part of the CLCA1 effect on mucus.

Fixed sections from control, rCLCA1, and CCh treated tissues were stained with Alcian blue/Periodic acid–Schiff (AB-PAS) to analyze if rCLCA1 induced mucus secretion (Fig. 4c). CCh treated tissue had dilated lower crypts (Fig. 4c, filled arrowhead) and reduced upper crypt goblet cell size (Fig. 4c, open arrowhead) compared to control tissue indicating increased mucus secretion in accordance with a previous report [27]. No difference could be observed between control and rCLCA1 treated tissue.

Since CLCA1 has repeatedly been reported to affect membrane ion currents when expressed *in vitro* [17–19,34], we further investigated the possibility that the mucus thickness increase induced by rCLCA1 treatment was mediated by altered ion transport across the epithelium. To address this we applied the Calcium activated chloride channel inhibitor CaCCinh A01, or the less specific inhibitors DIDS and NFA in combination with rCLCA1 (Fig. 4d). None of the ion channel inhibitors significantly affected the rCLCA1 response, supporting the conclusion that the rCLCA1 effect was not due to altered ion secretion.

3.6. CLCA1 is a Key Mediator of WT Mucus Expansion and it's Loss Is Compensated for by Cysteine-Proteases

We have previously shown that *Clca1*$^{-/-}$ mice do not have altered colonic mucus growth rate compared to WT *ex vivo* [13]. This seemed to contradict our result that CLCA1 is involved in the mucus growth when applied recombinantly. A possible explanation could be that *Clca1*$^{-/-}$ mice express and/or activate compensatory enzymes that mask the phenotype. We therefore investigated whether WT and *Clca1*$^{-/-}$ mucus growth responded differently to inhibitors of different protease classes. Metalloprotease inhibition by EDTA significantly decreased the mucus growth rate in WT but not in *Clca1*$^{-/-}$ mice

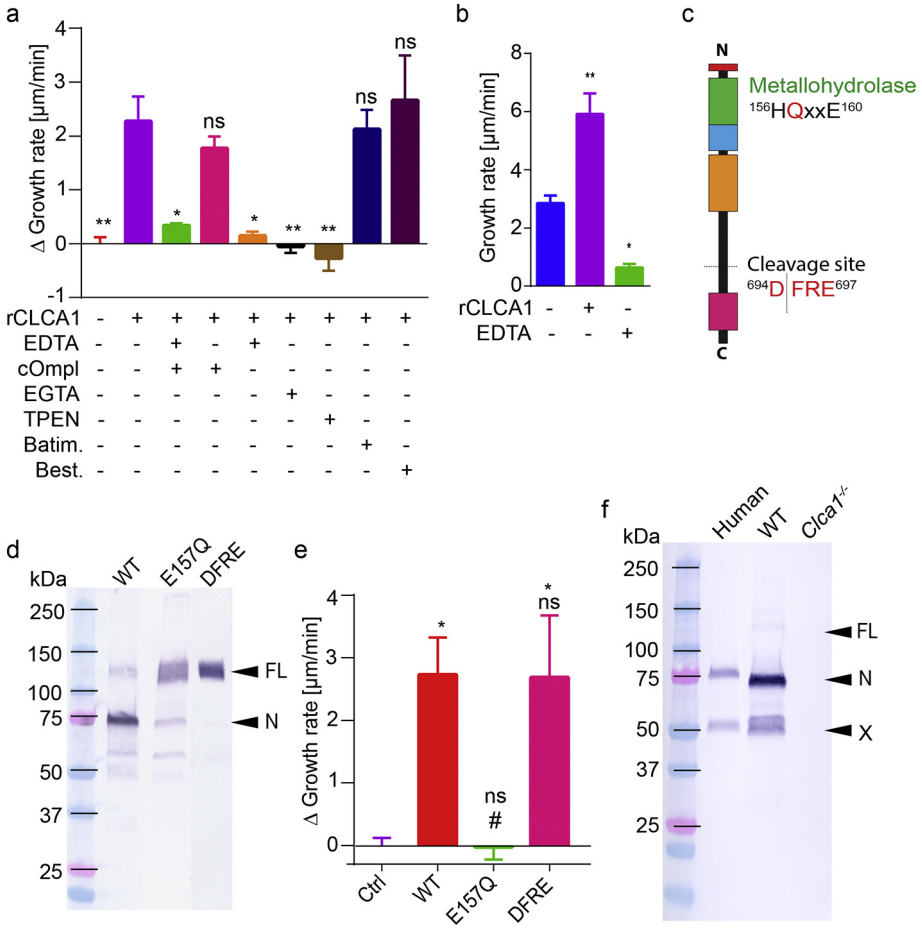

Fig. 3. CLCA1 acts as a metalloprotease to expand mucus. (a) The effect of rCLCA1 (5 μg) in combination with different protease inhibitors in *Clca1*$^{-/-}$ mucus presented as delta growth rate (growth rate of inhibitor + rCLCA treated mucus subtracted by the growth rate of inhibitor only treated mucus). Untreated and rCLCA1 alone treated mucus are also shown. cOmpl 1×, EDTA 10 mM, EGTA 10 mM, TPEN 1 mM, batimastat (Batim.) 200 μM, and bestatin (Best.) 130 μM ($n = 3–8$). (b) Mucus growth rate in untreated, rCLCA1 (5 μg) or EDTA (10 mM) treated human sigmoid colon biopsies (n = 3–4). (c) The metallohydrolase motif and the cleavage site are indicated on a schematic representation of CLCA1. (d) Western blot analysis of recombinantly expressed and purified CLCA1 with unmodified sequence (WT), p.E157Q protease null mutation (E157Q) and p.GALY694-697DFRE (DFRE) cleavage site mutation (representative of 4–7). FL = full-length CLCA1, N = N-terminal CLCA1 product. (e) Effect of rCLCA1 mutants (5 μg) on *Clca1*$^{-/-}$ mucus growth rate expressed as delta growth rate. Ctrl = control treated (PBS), WT = unmodified rCLCA1, E157Q = protease null p.E157Q mutant, DFRE = p.GALY694-697DFRE cleavage site mutant (n = 4–7). (f) Representative (of 5) western blot analysis of CLCA1 in human mucus and from wild-type (WT) and *Clca1*$^{-/-}$ mouse mucus. FL = full-length CLCA1, N = N-terminal CLCA1 product, X = 50 kDa N-terminal product of CLCA1. Data is presented as mean ± SEM; ns = non-significant, # or * $p \leq .05$, ** $p \leq .01$ as determined with one-way ANOVA followed by MCT (a: Dunnett's MCT *vs* only rCLCA1 treatment, b: Dunnett's MCT *vs* untreated, e: Tukey's MCT, * and # denote significance *vs* Ctrl and WT respectively).

(Fig. 5a). Conversely, inhibition of serine and cysteine proteases using cOmpl blocked mucus growth in *Clca1*$^{-/-}$ but had only minor effects in WT tissue, whereas treatment with both inhibitors blocked all growth in both genotypes. Together, this demonstrated that mucus growth in WT and *Clca1*$^{-/-}$ tissue was driven by different proteases and indicated that the enzyme inhibited by EDTA in WT mucus was CLCA1.

To further dissect if the effect of cOmpl was due to inhibition of cysteine or serine proteases we used the cysteine protease specific inhibitor E64-c. The effect of E64-c mimicked that of cOmpl in WT and *Clca1*$^{-/-}$ mucus respectively. This indicated that lack of CLCA1 in *Clca1*$^{-/-}$ mucus could be compensated for by cysteine-proteases, which mask the phenotype of altered mucus expansion.

3.7. CLCA1 is Involved in the Inner to Outer Mucus Layer Transition

Although the proteolytic activity of CLCA1 appeared to be compensated for in *Clca1*$^{-/-}$ mice, we speculated that differences in mucus structure could still be present. Mucus structural imaging was performed by staining explants with fluorescently tagged UEA1 which specifically binds to α1,2-fucose terminal O-glycan residues found on the MUC2 polymers in colon. Imaging explants from flushed colonic tissue (*i.e.* with the outer mucus layer removed) allowed visualization of the inner mucus layer in tissue from WT and *Clca1*$^{-/-}$ mice (Fig. 5b). This revealed condensed mucus at the mucus surface of *Clca1*$^{-/-}$ mice that were largely absent from WT controls. Closer examination of the WT mucus surface (Fig. 5c) demonstrated a regular, *net*-like material that resembled the theoretical structure of the extended MUC2 polymer [35]. The *Clca1*$^{-/-}$ mucus surface was on the other hand more irregular and covered by thick strands of mucus. Impaired mucus expansion resulting in condensed mucus clumps was quantified by mapping isosurfaces to UEA1 fluorescence (Fig. 5d), which was significantly higher (8-fold) in *Clca1*$^{-/-}$ compared to WT mice (Fig. 5e). This indicated that loss of CLCA1 resulted in limited expansion and alterations in the mucus structure.

As CLCA1 was shown to be important for expanding the mucus its effect on the mucus organization was studied. Explants were prepared from unflushed colonic tissue and stained to detect luminal mucus and mucosal bacteria (Fig. 5f). In WT explants stratified mucus was clearly observed at the inner/outer mucus interface (arrows) (Fig. 5f, blue boxes) and more voluminous expanded mucus luminal to this. Conversely the inner/outer layer interface in *Clca1*$^{-/-}$ explants was poorly defined and the outer layer appeared to be composed of condensed mucus strands. In both WT and *Clca1*$^{-/-}$ explants most bacteria were observed in the outer mucus away from the epithelium (Fig. 5F

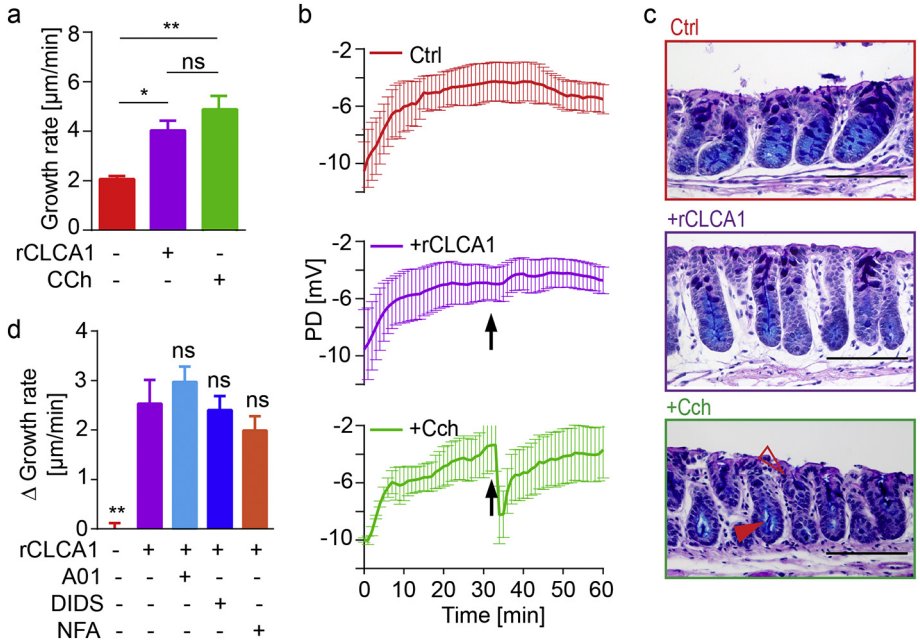

Fig. 4. CLCA1 does not mediate its effect by mucus or ion secretion. (a) Mucus growth rate measured in untreated, rCLCA1 (5 μg), and CCh (1 mM) treated mucus from *Clca1*$^{-/-}$ mice (n = 5–7). (b) Transepithelial potential difference (PD) was recorded in untreated (Ctrl, red), rCLCA1 (purple), and CCh (green) treated *Clca1*$^{-/-}$ tissues. Treatments were added at t = 32 min (arrow) (n = 4). (c) Representative AB-PAS stained sections from untreated (Ctrl), rCLCA1, and CCh treated *Clca1*$^{-/-}$ tissues. Dilated crypt bottoms (filled arrowhead) and emptied goblet cells at the crypt opening (open arrowhead) are indicated in CCh treated tissues. Scale bars are 100 μm (n = 5–7). (d) The effect of rCLCA1 (5 μg) in combination with different ion channel inhibitors on the mucus presented as delta growth rate (growth rate of inhibitor + rCLCA1 treated mucus subtracted by the average growth rate of inhibitor only treated mucus). Values for untreated and rCLCA1 alone treated mucus are also shown. CaCCinh A01 (A01) 100 μM, DIDS 200 μM, and NFA 300 μM. N = 4–5. Denoted significances *vs* only rCLCA1 treatment. Data is presented as mean ± SEM; ns = non-significant, * p ≤ .05, ** p ≤ .01 with one-way ANOVA with Tukey's MCT.

yellow boxes). Together, this indicates that CLCA1 is involved in regulation of the normal transition between the inner and outer mucus layer.

4. Discussion

Inhibition of colonic mucus growth upon treatment with metalloprotease inhibitors suggested that mucus dynamics in colon is, at least partly, dependent on metalloprotease activity. As the effect of EDTA was similar in both Conv-R and GF mice, we concluded that the proteases are endogenous to the animals. The most abundant mucus protein harboring a hydrolase domain is CLCA1, one of the five most abundant mucus proteins in both human and mouse colonic mucus, which led us to investigate the involvement of CLCA1 in mucus processing. We have previously described how *Clca1*$^{-/-}$ mice lack an apparent mucus phenotype [13]. We therefore continued to investigate the function of CLCA1 by measuring the effect of rCLCA1 on secreted mucus on colonic explants. Addition of rCLCA1 increased the mucus thickness with greater penetrability in the uppermost mucus. The expanded penetrable mucus must be formed from the inner non-penetrable mucus layer by processes that will change the mucus structure. That this process acts on the luminal side of the inner mucus is supported by the finding that the mobility right above the inner mucus surface is decreased. This would form a gradient of processed mucus with higher density closest to the inner mucus layer surface. As we did not observe any signs of increased mucus secretion, altered transepithelial potential difference, or effect of ion channel inhibitors on rCLCA1 treatment [36, 37] we ruled out a role for CLCA1 in mucus secretion and ion transport to modulate mucus. The observed increased mucus growth rate was thus likely mediated by proteolysis resulting in mucus expansion. Importantly, the results regarding CLCA1 from mouse intestine were translatable to human colon biopsies which confirm the conservation of CLCA1 as a mucus processing enzyme.

The inability of ion channel inhibitors to block the rCLCA1 effect was somewhat surprising considering the large number of reports supporting a connection between CLCA1 and chloride transport [17–19, 38]. However, these studies were based on *in vitro* experiments and in contrast to an *in vivo* study by Mundhenk et al. concluding that CLCA1 does not contribute to chloride conductance in mouse airways [25].

The CLCA1 mediated increase in mucus growth was evident from both mucus thickness measurements and confocal bead assays. The effect could be inhibited by divalent cation chelating agents such as EDTA and TPEN, but these agents could also have other effects on the system. However, no observed effects in *Clca1*$^{-/-}$ mice upon treatment argue for a specific CLCA1 effect. Inhibition by TPEN also indicates a Zn^{2+} dependent effect and inactivity of the rCLCA1 protease null mutant supports proteolytic processing as the mechanism. Batimastat, a hydroxamate-based MMP inhibitor previously shown to inhibit CLCA1 autocatalytic activity [18] did not have any effect on rCLCA1 in our system. The short experimental times used could influence this, but a related inhibitor, Marimastat, has also been shown not to affect CLCA1 [21]. Despite similarities to MMP and ADAMs, this implies that CLCA1 seems to be part of a different, as yet uncharacterized metalloprotease family.

Enzymes are usually found in much lower amounts compared to their substrate. The high concentration of CLCA1 in mucus suggests that its enzymatic activity is tightly regulated. This is supported by the ability of exogenous rCLCA1 to induce increased mucus growth in WT mucus that already contains high levels of endogenous CLCA1. The autocatalytic cleavage of CLCA1 has been suggested as a regulatory mechanism [18], but as the uncleaved p.GALY694-697DFRE rCLCA1 mutant gave the same response as rCLCA1, and we only detected fully processed CLCA1 in both human and mouse mucus we find this less likely. However, identification of an approximately 50 kDa N-terminal CLCA1 derived protein product in the mucus suggests that further processing of CLCA1 could be involved in its regulation. A similarly sized product was also observed in a previous study strengthening this hypothesis [39]. However, other means of regulation may also exist, such as

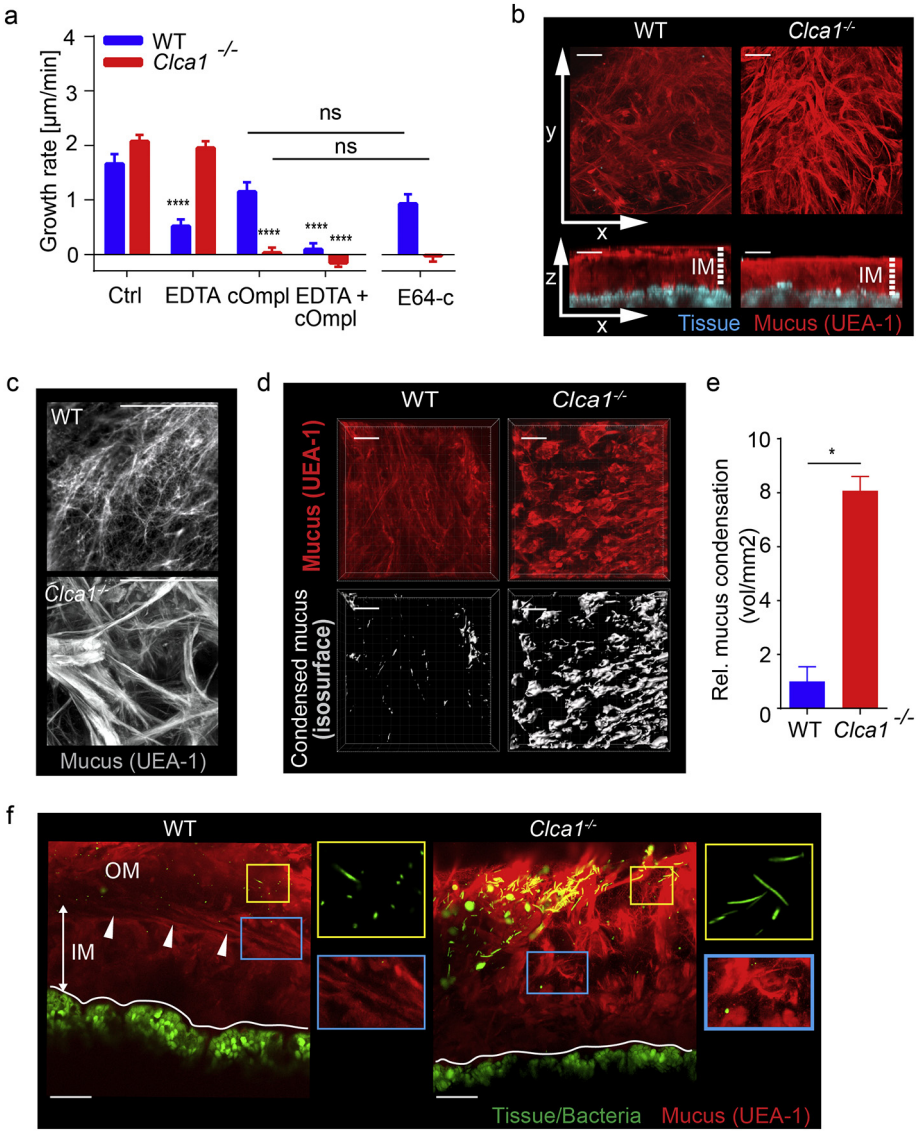

Fig. 5. The effect of CLCA1 on the mucus structure. (a) The effect of different classes of protease inhibitors on WT (blue) and *Clca1*$^{-/-}$ (red) mucus growth rate. EDTA 10 mM, cOmpl 1×, E64-c 20 μM (n = 3–5). * denotes significance to Ctrl within each genotype, or as indicated by brackets. (b) Flushed distal colon explants from WT and *Clca1*$^{-/-}$ mice were stained with fluorescent UEA1 lectin (red) to visualize the mucus. Images were acquired by confocal microscopy in z-stacks represented by x/y-axis (upper panels) and x/z-axis (lower panels). White arrows indicate axis direction; dashed lines indicate inner mucus (IM). (c) Magnified view of the mucus surface from *ex vivo* UEA1 lectin (grey) stained colonic mucus from WT and *Clca1*$^{-/-}$ mice. (d) Mucus on flushed tissue stained with UEA1 were used to map isosurfaces as a measure of clumped mucus. (e) Detection of clumped mucus was quantified by mapping isosurfaces to a threshold level of UEA1 fluorescence. (f) Images of unflushed explants stained with UEA1 to detect mucus and Syto-9 to detect mucosal bacteria on WT and *Clca1*$^{-/-}$ mouse colon explants. White lines indicate tissue surface; white arrows indicate the interface between the inner (IM) and outer (OM) mucus layers. Right panels show magnified images of mucosal bacteria (yellow boxes) and the IM/OM interface (blue boxes). Data is presented as mean ± SEM of 3–5 (a) or 4 per group (b-f) animals; ns = non-significant, *p ≤ .05, ****p ≤ .0001 as determined with two-way ANOVA followed by Tukey's MCT (A) or by Mann-Whitney test (e). All figure scale bars are 50 μm.

changes in conformation upon pH or redox potential alterations, or binding of co-factors. Furthermore, the high abundance of CLCA1 could also indicate additional functions for this protein.

Any substrate for CLCA1 has not yet been identified, but structural components in the mucus, like the main structural network protein MUC2, would be the most probable candidates. Cleavages in the terminal parts of MUC2 could lead to structural changes that would increase the volume without disrupting the disulphide bond stabilized network [40]. Investigation of the mucus structure at the inner to outer mucus transition zone using *ex vivo* lectin staining revealed that lack of CLCA1 resulted in denser MUC2 oligomers, supporting the idea that MUC2 would serve as a substrate for CLCA1. We have however so far not been able to confirm this *in vitro*. Further, although CLCA1 is primarily expressed by the intestine it has also been reported to be expressed in stomach, uterus and testis in healthy objects, and in diseased lung, which are all covered by mucus suggesting that the role of CLCA1 is associated with mucus, but is not restricted to colon [23, 41].

The fact that the mucus expansion phenotype in *Clca1*$^{-/-}$ mice is masked by a cysteine proteases activity highlights a redundancy in the mucus processing system. A role for CLCA homologs as murine CLCA4 or CLCA6 could be suggested [24, 25], but as EDTA had no effect on mucus growth in *Clca1*$^{-/-}$ mice, and our mucus proteome results does not support this [13], we find it less likely.

We believe that the herein described CLCA1 mediated mucus expansion is a key element in mucus transformation from attached dense inner mucus into loose outer mucus and by this allows smooth distal transport of luminal material [5]. Whether the activity of CLCA1 is spatially enriched at the inner-to-outer mucus layer transition zone or if CLCA1 is found throughout the mucus layer is so far unclear, although the distribution of CLCA1 in the mucus layer seen with IHC suggests

the latter. It is possible that CLCA1 processes the mucus structure continuously, but that a threshold is reached at a certain distance from the tissue that results in the inner-to-outer mucus layer conversion. A cascade reaction could be envisioned. Tight regulation of CLCA1's activity could also play a role. Alternatively, if CLCA1 requires either further proteolytic processing of itself for activity, or requires pre-processing of its substrate by other enzymes, these events could be restricted to the transition zone. Regulation of CLCA1 by endogenous inhibitors is another possible mechanism. Further characterization of CLCA1 activity and processing will hopefully shed light on all of this.

In line with our proposal of CLCA1 being involved in the processing of intestinal mucus to facilitate distal transport of mucus and luminal material, transgenic restoration of CLCA1 in a CF-model with reduced CLCA1 expression in the small intestine ameliorated the mucus obstruction phenotype and thereby increased the survival of the transgenic mice [42]. A CLCA1 variant has also been associated with meconium ileus in CF patients [43]. In light of the result presented here, this could be explained by increased proteolytic processing of the entrapped mucus. Further, CLCA1 could, by expanding the mucus, be envisioned to play a role in clearance of secreted mucus during intestinal infection *e.g.* by helminths. In agreement with this, CLCA1 has been shown to be upregulated in response to both *Trichinella spiralis* and *Trichuris muris* [44,45]. Induction, or failed induction, of CLCA1 could possibly also account for resistance or susceptibility against parasitic infection [46], although this has not been tested in greater detail but remains an interesting future study to determine.

Stagnant mucus and bacterial infections are also known to be associated with airway diseases such as CF, asthma and COPD [42]. The proposed role for the induced CLCA1 expression seen in T_H2-type asthma and COPD is to mediate goblet cell hyperplasia and mucin overproduction typical for these diseases (reviewed in [23]). However, the precise mechanism of CLCA1 in this context is still not fully understood and the literature is contradictory [25, 47–50]. Our results show a different role for CLCA1 in colonic mucus and we hope that the role for CLCA1 as a mucus processing metalloprotease will be addressed in future studies.

In conclusion, the presented work shows that endogenous metalloprotease activity is a key mediator of intestinal mucus processing. Further, we have been able to identify CLCA1 as a main contributor to this activity which is independent of ion or mucus secretion from the epithelium. The observation that CLCA1 seems to be involved in the conversion from the firm inner mucus layer to the loose outer mucus layer indicates that CLCA1 facilitates removal of mucus which is important for mucus homeostasis. However, further studies will have to address the physiological targets and effects of CLCA1 protease activity. As the function of CLCA1 seems to be conserved between human and mouse, better knowledge of CLCA1 function in relation to mucus removal is potentially of great importance for better understanding of human pathology and development of new drug targets in diseases with mucus defects.

Supplementary data to this article can be found online at https://doi.org/10.1016/j.ebiom.2018.05.031.

Acknowledgement

We acknowledge F. Hoffman-La Roche for providing the mClca3$^{-/-}$ mouse strain (here called Clca1$^{-/-}$), and Professor Fredrik Bäckhed for providing germ free animals. We thank the Mammalian Protein Expression and Centre for Cellular Imaging Core Facilities for their assistance.

Funding Sources

This work was supported by the Swedish Research Council, The Swedish Cancer Foundation, The Hasselblad foundation, The Knut and Alice Wallenberg Foundation, National Institute of Allergy and Infectious Diseases (U01AI095473, the content is solely the responsibility of the authors and does not necessarily represent the official views of the NIH), IngaBritt and Arne Lundberg Foundation, Sahlgren's University Hospital (ALF), Wilhelm and Martina Lundgren's Foundation, and The Sahlgrenska Academy.

Conflict of Interest

The authors declare that they have no conflict of interest.

Author Contributions

MEVJ and EELN conceived the original idea and planned the study; EELN, GMHB, SvdP and LA, designed and performed different experiments; EELN, GMHB and LA analyzed the data; MEVJ and GCH supervised the study; ADG provided experimental material, models and discussions; EELN and MEVJ wrote the manuscript with input from all authors.

References

[1] Johansson ME, Sjovall H, Hansson GC. The gastrointestinal mucus system in health and disease. Nat Rev Gastroenterol Hepatol 2013;10:352–61.
[2] Sharpe C, Thornton DJ, Grencis RK. A sticky end for gastrointestinal helminths; the role of the mucus barrier. Parasite Immunol 2018;40:e12517.
[3] Munck A. Cystic fibrosis: evidence for gut inflammation. Int J Biochem Cell Biol 2014;52:180–3.
[4] Thornton DJ, Rousseau K, McGuckin MA. Structure and function of the polymeric mucins in airways mucus. Annu Rev Physiol 2008;70:459–86.
[5] Johansson ME, Phillipson M, Petersson J, Velcich A, Holm L, Hansson GC. The inner of the two Muc2 mucin-dependent mucus layers in colon is devoid of bacteria. Proc Natl Acad Sci U S A 2008;105:15064–9.
[6] Ambort D, Johansson ME, Gustafsson JK, Nilsson HE, Ermund A, Johansson BR, et al. Calcium and pH-dependent packing and release of the gel-forming MUC2 mucin. Proc Natl Acad Sci U S A 2012;109:5645–50.
[7] Birchenough GM, Nystrom EE, Johansson ME, Hansson GC. A sentinel goblet cell guards the colonic crypt by triggering Nlrp6-dependent Muc2 secretion. Science 2016;352:1535–42.
[8] Johansson ME, Gustafsson JK, Sjoberg KE, Petersson J, Holm L, Sjovall H, et al. Bacteria penetrate the inner mucus layer before inflammation in the dextran sulfate colitis model. PLoS ONE 2010;5:e12238.
[9] Johansson ME, Gustafsson JK, Holmen-Larsson J, Jabbar KS, Xia L, Xu H, et al. Bacteria penetrate the normally impenetrable inner colon mucus layer in both murine colitis models and patients with ulcerative colitis. Gut 2014;63:281–91.
[10] Johansson ME, Jakobsson HE, Holmen-Larsson J, Schutte A, Ermund A, Rodriguez-Pineiro AM, et al. Normalization of host intestinal mucus layers requires long-term microbial colonization. Cell Host Microbe 2015;18:582–92.
[11] Schutte A, Ermund A, Becker-Pauly C, Johansson ME, Rodriguez-Pineiro AM, Backhed F, et al. Microbial-induced meprin beta cleavage in MUC2 mucin and a functional CFTR channel are required to release anchored small intestinal mucus. Proc Natl Acad Sci U S A 2014;111:12396–401.
[12] Gustafsson JK, Ermund A, Ambort D, Johansson ME, Nilsson HE, Thorell K, et al. Bicarbonate and functional CFTR channel are required for proper mucin secretion and link cystic fibrosis with its mucus phenotype. J Exp Med 2012;209:1263–72.
[13] Erickson NA, Nystrom EE, Mundhenk L, Arike L, Glauben R, Heimesaat MM, et al. The goblet cell protein Clca1 (alias mClca3 or Gob-5) is not required for intestinal mucus synthesis, structure and barrier function in naive or DSS-challenged mice. PLoS ONE 2015;10:e0131991.
[14] Rodriguez-Pineiro AM, Bergstrom JH, Ermund A, Gustafsson JK, Schutte A, Johansson ME, et al. Studies of mucus in mouse stomach, small intestine, and colon. II. Gastrointestinal mucus proteome reveals Muc2 and Muc5ac accompanied by a set of core proteins. Am J Physiol Gastrointest Liver Physiol 2013;305:G348–56.
[15] Agnel M, Vermat T, Culouscou JM. Identification of three novel members of the calcium-dependent chloride channel (CaCC) family predominantly expressed in the digestive tract and trachea. FEBS Lett 1999;455:295–301.
[16] Gruber AD, Elble RC, Ji HL, Schreur KD, Fuller CM, Pauli BU. Genomic cloning, molecular characterization, and functional analysis of human CLCA1, the first human member of the family of Ca2+−activated cl- channel proteins. Genomics 1998;54:200–14.
[17] Sala-Rabanal M, Yurtsever Z, Nichols CG, Brett TJ. Secreted CLCA1 modulates TMEM16A to activate Ca-dependent chloride currents in human cells. Elife 2015;4.
[18] Yurtsever Z, Sala-Rabanal M, Randolph DT, Scheaffer SM, Roswit WT, Alevy YG, et al. Self-cleavage of human CLCA1 protein by a novel internal metalloprotease domain controls calcium-activated chloride channel activation. J Biol Chem 2012;287:42138–49.
[19] Hamann M, Gibson A, Davies N, Jowett A, Walhin JP, Partington L, et al. Human ClCa1 modulates anionic conduction of calcium-dependent chloride currents. J Physiol 2009;587:2255–74.
[20] Mundhenk L, Alfalah M, Elble RC, Pauli BU, Naim HY, Gruber AD. Both cleavage products of the mCLCA3 protein are secreted soluble proteins. J Biol Chem 2006;281:30072–80.

[21] Bothe MK, Mundhenk L, Kaup M, Weise C, Gruber AD. The murine goblet cell protein mCLCA3 is a zinc-dependent metalloprotease with autoproteolytic activity. Mol Cells 2011;32:535–41.
[22] Pawlowski K, Lepisto M, Meinander N, Sivars U, Varga M, Wieslander E. Novel conserved hydrolase domain in the CLCA family of alleged calcium-activated chloride channels. Proteins 2006;63:424–39.
[23] Patel AC, Brett TJ, Holtzman MJ. The role of CLCA proteins in inflammatory airway disease. Annu Rev Physiol 2009;71:425–49.
[24] Patel AC, Morton JD, Kim EY, Alevy Y, Swanson S, Tucker J, et al. Genetic segregation of airway disease traits despite redundancy of calcium-activated chloride channel family members. Physiol Genomics 2006;25:502–13.
[25] Mundhenk L, Johannesson B, Anagnostopoulou P, Braun J, Bothe MK, Schultz C, et al. mCLCA3 does not contribute to calcium-activated chloride conductance in murine airways. Am J Respir Cell Mol Biol 2012;47:87–93.
[26] Gustafsson JK, Ermund A, Johansson ME, Schutte A, Hansson GC, Sjovall H. An ex vivo method for studying mucus formation, properties, and thickness in human colonic biopsies and mouse small and large intestinal explants. Am J Physiol Gastrointest Liver Physiol 2012;302:G430–8.
[27] Gustafsson JK, Linden SK, Alwan AH, Scholte BJ, Hansson GC, Sjovall H. Carbachol-induced colonic mucus formation requires transport via NKCC1, K(+) channels and CFTR. Pflugers Arch 2015;467:1403–15.
[28] Vizcaino JA, Deutsch EW, Wang R, Csordas A, Reisinger F, Rios D, et al. ProteomeXchange provides globally coordinated proteomics data submission and dissemination. Nat Biotechnol 2014;32:223–6.
[29] Wisniewski JR, Zougman A, Nagaraj N, Mann M. Universal sample preparation method for proteome analysis. Nat Methods 2009;6:359–62.
[30] van der Post S, Hansson GC. Membrane protein profiling of human colon reveals distinct regional differences. Mol Cell Proteomics 2014;13:2277–87.
[31] Cox J, Mann M. MaxQuant enables high peptide identification rates, individualized p.p.b.-range mass accuracies and proteome-wide protein quantification. Nat Biotechnol 2008;26:1367–72.
[32] Cox J, Neuhauser N, Michalski A, Scheltema RA, Olsen JV, Mann M. Andromeda: a peptide search engine integrated into the MaxQuant environment. J Proteome Res 2011;10:1794–805.
[33] Bergstrom JH, Birchenough GM, Katona G, Schroeder BO, Schutte A, Ermund A, et al. Gram-positive bacteria are held at a distance in the colon mucus by the lectin-like protein ZG16. Proc Natl Acad Sci U S A 2016;113:13833–8.
[34] Loewen ME, Bekar LK, Gabriel SE, Walz W, Forsyth GW. pCLCA1 becomes a cAMP-dependent chloride conductance mediator in Caco-2 cells. Biochem Biophys Res Commun 2002;298:531–6.
[35] Ambort D, Johansson ME, Gustafsson JK, Ermund A, Hansson GC. Perspectives on mucus properties and formation—lessons from the biochemical world. Cold Spring Harb Perspect Med 2012;2.
[36] Liu Y, Zhang H, Huang D, Qi J, Xu J, Gao H, et al. Characterization of the effects of cl(−) channel modulators on TMEM16A and bestrophin-1 ca(2)(+) activated cl(−) channels. Pflugers Arch 2015;467:1417–30.
[37] Gandhi R, Elble RC, Gruber AD, Schreur KD, Ji HL, Fuller CM, et al. Molecular and functional characterization of a calcium-sensitive chloride channel from mouse lung. J Biol Chem 1998;273:32096–101.
[38] Sala-Rabanal M, Yurtsever Z, Berry KN, Nichols CG, Brett TJ. Modulation of TMEM16A channel activity by the von Willebrand factor type a (VWA) domain of the calcium-activated chloride channel regulator 1 (CLCA1). J Biol Chem 2017;292:9164–74.
[39] Leverkoehne I, Gruber AD. The murine mCLCA3 (alias gob-5) protein is located in the mucin granule membranes of intestinal, respiratory, and uterine goblet cells. J Histochem Cytochem 2002;50:829–38.
[40] Johansson ME, Larsson JM, Hansson GC. The two mucus layers of colon are organized by the MUC2 mucin, whereas the outer layer is a legislator of host–microbial interactions. Proc Natl Acad Sci U S A 2011;108(Suppl. 1):4659–65.
[41] Behera SK, Praharaj AB, Dehury B, Negi S. Exploring the role and diversity of mucins in health and disease with special insight into non-communicable diseases. Glycoconj J 2015;32:575–613.
[42] Young FD, Newbigging S, Choi C, Keet M, Kent G, Rozmahel RF. Amelioration of cystic fibrosis intestinal mucous disease in mice by restoration of mCLCA3. Gastroenterology 2007;133:1928–37.
[43] van der Doef HP, Slieker MG, Staab D, Alizadeh BZ, Seia M, Colombo C, et al. Association of the CLCA1 p.S357N variant with meconium ileus in European patients with cystic fibrosis. J Pediatr Gastroenterol Nutr 2010;50:347–9.
[44] Knight PA, Brown JK, Pemberton AD. Innate immune response mechanisms in the intestinal epithelium: potential roles for mast cells and goblet cells in the expulsion of adult Trichinella spiralis. Parasitology 2008;135:655–70.
[45] Datta R, deSchoolmeester ML, Hedeler C, Paton NW, Brass AM, Else KJ. Identification of novel genes in intestinal tissue that are regulated after infection with an intestinal nematode parasite. Infect Immun 2005;73:4025–33.
[46] Gossner A, Wilkie H, Joshi A, Hopkins J. Exploring the abomasal lymph node transcriptome for genes associated with resistance to the sheep nematode Teladorsagia circumcincta. Vet Res 2013;44:68.
[47] Alevy YG, Patel AC, Romero AG, Patel DA, Tucker J, Roswit WT, et al. IL-13-induced airway mucus production is attenuated by MAPK13 inhibition. J Clin Invest 2012;122:4555–68.
[48] Robichaud A, Tuck SA, Kargman S, Tam J, Wong E, Abramovitz M, et al. Gob-5 is not essential for mucus overproduction in preclinical murine models of allergic asthma. Am J Respir Cell Mol Biol 2005;33:303–14.
[49] Nakanishi A, Morita S, Iwashita H, Sagiya Y, Ashida Y, Shirafuji H, et al. Role of gob-5 in mucus overproduction and airway hyperresponsiveness in asthma. Proc Natl Acad Sci U S A 2001;98:5175–80.
[50] Thai P, Chen Y, Dolganov G, Wu R. Differential regulation of MUC5AC/Muc5ac and hCLCA-1/mGob-5 expression in airway epithelium. Am J Respir Cell Mol Biol 2005;33:523–30.